

# OTFS MODULATION FOR THE AMT ENVIRONMENT

Richard Simeon

Department of Electrical Engineering and Computer Science

The University of Kansas

Lawrence, KS, 66045

rsimeon@ku.edu

Faculty Advisor:

Dr. Erik Perrins

## ABSTRACT

Orthogonal Time Frequency Space (OTFS) is a new modulation designed to operate in the high-mobility/high-Doppler environment that is closely related to 5G's Orthogonal Frequency Division Multiplexing (OFDM). OFDM has been investigated for use in the next generation telemetry systems, but performance can suffer at high test article (TA) speeds due to rapid variations in the time-frequency channel response and inter-carrier interference (ICI) resulting from Doppler shifts.

This paper presents an overview of OTFS and an exemplary OTFS system that can operate at high TA speeds in the Aeronautical Mobile Telemetry (AMT) environment to showcase advantages over OFDM such as resistance to ICI and jamming, lower peak to average power ratio (PAPR), and better spectral efficiency. Future areas of research unique to the AMT use case are discussed.

## INTRODUCTION

AMT data consumption has been growing exponentially since 1972 [1]. It is projected that by 2030 data rate needs will exceed 1Gbps. With spectrum allocations scarce, the need for higher spectral efficiencies is key to meeting the projected demand. OFDM has been investigated to augment the existing single-carrier based continuous phase modulation (CPM) systems in use today for the next generation Integrated Network Enhanced Telemetry (iNET) Telemetry Network System. The use of cellular-based communications systems for telemetry is known as Cellular Range Telemetry (CRTM). Even though OFDM has been proven to be successful in cellular based communications systems such as WiFi, LTE, and 5G, the modulation scheme suffers at GHz frequencies when subjected to high Doppler shifts relative to the OFDM subcarrier spacing and in the presence of multipath fading.

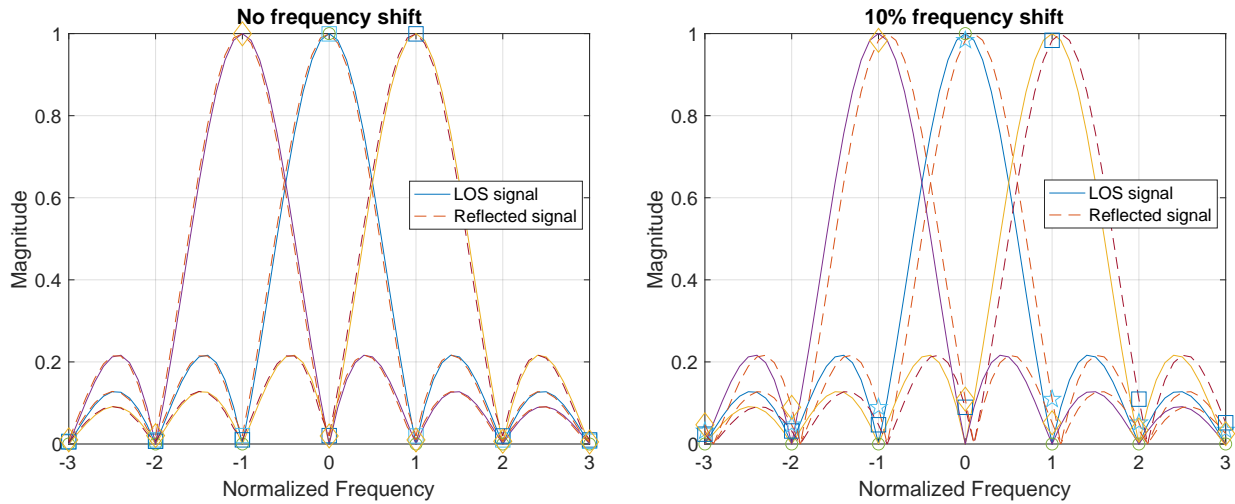
The implementation and challenges of LTE in the AMT environment has been extensively covered. Henceforth we refer to the TA as having a transceiver similar to a mobile user equipment (UE) in

LTE parlance. In [2] the author listed the challenges of commercial off-the-shelf (COTS) LTE in the AMT environment such as the large uplink traffic (opposite of typical terrestrial traffic flows) and the high-speed/high Doppler environment that impacts the subcarrier orthogonality in OFDM (i.e. ICI). The challenge of large Doppler compensation was discussed in [3] and a solution using a front-end Doppler compensator between the RF front-end and the LTE modem was proposed in [4], simulated in [5], and tested in [6]. In [7] the author recognizes that a CRTM-based system must involve handovers from one cell to another that require the mobile user equipment (UE) to measure neighboring cells with differing Doppler shifts for signal quality metrics. Handovers in [3] were accomplished when the TA senses a low-Doppler neighbor cell, which occurs when the TA is approximately overhead of the cell antenna. However, handovers typically occur at the cell edges where the low signal strengths and disparate Doppler frequencies between the serving cell and neighbor cells compromise the accuracy of the signal quality measurements, and remains an open challenge in OFDM-based systems.

OTFS is a multicarrier two-dimensional modulation scheme that was introduced in [8] as a solution to meet the goal of higher-speed mobile communications desired by the 3GPP international standards body for Beyond-5G (B5G) and 6G systems. Whereas OFDM operates in the time-frequency (TF) domain, OTFS operates in the delay-Doppler (DD) domain. Assuming a mobile channel with a few scatterers, the time-variant channel in the TF domain is transformed into a quasi-static and sparse time-invariant channel in the DD domain. This property has benefits with respect to channel stationarity (less overhead needed for channel estimation) and receiver decoding (sparsity in the channel can be exploited). In certain conditions, OTFS can be viewed as block precoding of OFDM, since symbols are processed in the DD domain that can be transformed into the familiar TF domain.

The unique advantages of OTFS in high-Doppler environments makes this modulation suitable for AMT. This paper presents the case for using OTFS in the AMT environment. We start by explaining the challenges of OFDM in the AMT environment. We then describe the high-mobility multipath channel in the time and time-frequency domain. The delay-Doppler domain is then introduced along with the channel characteristics in that domain. We introduce OTFS to modulate symbols in the delay-Doppler domain, discuss its advantages over OFDM, then present an exemplary cellular-based range telemetry (CRTM) system using OTFS that is suitable for high-speed AMT. Of particular emphasis in the design is the emphasis on intra-cell handovers, which can be problematic in OFDM at high speeds due to severe Doppler offsets, but manageable in OTFS.

*Notation:* A bold lower case  $\mathbf{a}$  and bold upper case  $\mathbf{A}$  is a column vector and matrix, respectively.  $a$  is a scalar,  $\mathbf{a}[i]$  is the  $i$ th entry of  $\mathbf{a}$ ,  $\mathbf{A}(i)$  is the  $i$ th column, and  $\mathbf{A}[i, j]$  or  $\mathbf{A}_{ij}$  is the  $i$ th row and  $j$ th column entry of  $\mathbf{A}$ . All matrix and vector indices start at zero.  $\hat{a}$  and  $|a|$  are the estimate and the absolute value of  $a$ .  $|\cdot|_M$ ,  $\lfloor \cdot \rfloor$ , and  $\delta(\cdot)$  are the modulo  $M$ , floor operator, and Kronecker delta function, respectively.  $\mathbf{A} \circledast \mathbf{B}$  is the circular convolution operation.



(a) Subcarrier orthogonality.

(b) ICI caused by Doppler-shifted path.

Figure 1: OFDM subcarrier spectrum in normal and ISI conditions.

## DOPPLER EFFECTS ON OFDM

The phenomena of OFDM degradation in Doppler channels is well-known [9]. OFDM divides the channel into  $M$  parallel subcarriers that each transmit complex-valued signals representing a QAM alphabet. When rectangular pulse shaping is used, each subcarrier has a sinc-shaped frequency spectrum where the nulls of the sinc pulse fall on the center frequencies of adjacent subcarriers (as shown in fig. 1a). This makes transmissions on each subcarrier orthogonal to the other subcarriers.

When some scatterers have a different Doppler shift than the line of sight (LOS) path, their subcarrier nulls no longer coincide with adjacent subcarriers and the orthogonality of the sinc pulses between the main LOS path and the reflected path no longer holds. Fig. 1b shows the spectrum of a reflected path Doppler-shifted in frequency. The nulls of the sinc pulse from the shifted spectrum do not fall on the centers of the other LOS subcarriers, so subcarrier orthogonality is lost and there is signal leakage into the neighboring subcarriers. This leakage results in inter-carrier interference (ICI). Doppler shifts at vehicular speeds are a small fraction of the subcarrier spacing, so ICI is typically negligible. However, speeds on high-speed trains and aircraft induce large Doppler shifts that can make ICI the dominant source of noise.

## THE HIGH-MOBILITY MULTIPATH CHANNEL

The communications channel is traditionally represented as a tapped delay line (TDL) acting as an FIR filter on the transmitted signal where each tap is from a scatterer such as a building, car, etc. The filtering effect causes *frequency-selective fading* which distorts the transmitted signal by varying the channel gain at different frequencies, and its effects must be undone at the receiver. Use

of subcarriers in OFDM combat the frequency-selective fading if the distortion is known through channel state information (CSI) measurements. The length of time spanned by the TDL is called the *delay spread*.

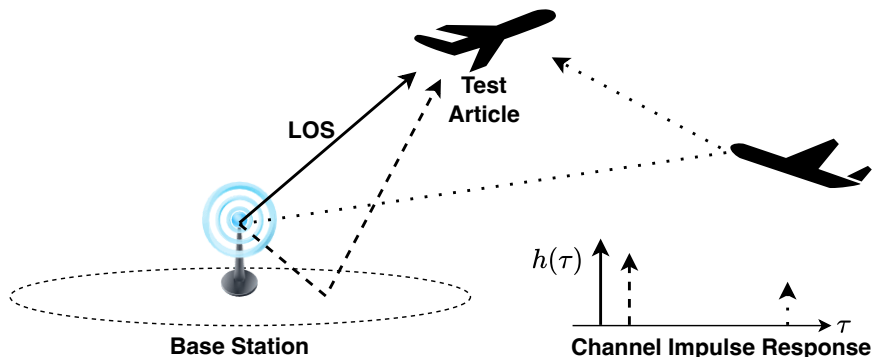


Figure 2: Multipath channel.

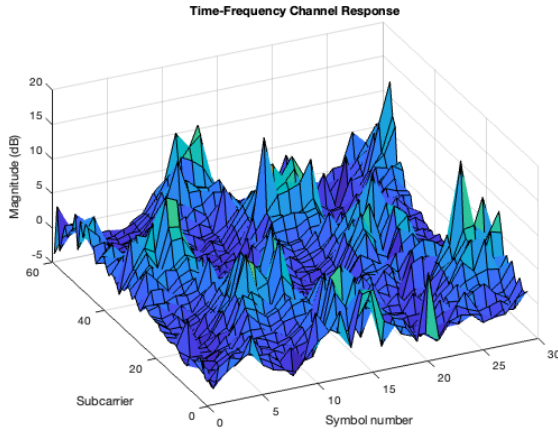
3GPP channel propagation models typically represent scenarios such as urban environments using two parameters: the excess tap delay  $\tau$  (where the first tap is at  $\tau = 0$ ) and the mean complex-valued tap gain  $h(\tau)$ . Fig. 2 shows an example of a channel between a base station (BS) and TA with two scatterers and a line-of-sight (LOS) path. Together the physical paths effectively form a three-tap FIR filter acting between the BS and TA. Any Doppler shift imposed on the path is represented as a Doppler frequency-modulated path gain.

If the TA is stationary, the channel is linear and time-invariant (LTI) and these two parameters are sufficient to describe a one-dimensional channel impulse response (CIR). However, if the TA is moving, propagation path delays change which causes time-varying constructive and destructive interference at the TA that affect the TDL tap amplitudes. Thus the channel is time-varying with a rate proportional to that of the TA velocity. The mobile channel description is now a two-dimensional CIR where the parameters are the time  $t$ , excess delay  $\tau$ , and the complex gain  $h(t, \tau)$ . The amount of time that the channel appears to be stationary is called the *coherence time* and is inversely proportional to velocity (Doppler spread). The combination of frequency-selective fading (from the multiple channel taps) and time-varying fading (from the movement of the TA) is typically called a *doubly-dispersive* or *doubly-selective* channel.

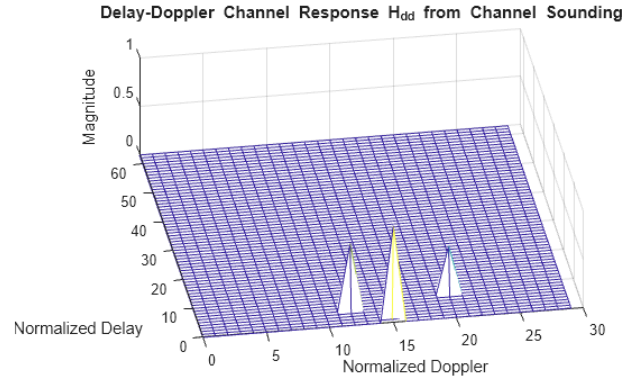
CSI measurements are typically done by transmitting a known (*pilot*) signal and observing the distortion at the receiver to determine the channel parameters that caused the distortion. Channel estimation must be done at intervals smaller than the coherence time to obtain fresh CSI for receiver distortion compensation. Since pilot signals replace data symbols, effective throughput suffers and the spectral efficiency (SE) of the system decreases. Thus it is important that CSI estimates are done as infrequently as possible.

#### A. The Time-Frequency Channel Representation

The TDL is a simple time-domain representation of the channel. However, the channel can be described in other useful domains. OFDM operates in the time-frequency (TF) domain. The



(a) Time-frequency channel response.



(b) Delay-Doppler channel response.

Figure 3: Channel responses in different domains for the same doubly-dispersive channel.

complex gain  $h(f, t)$  describes the channel gain in the TF domain at time  $t$  and frequency  $f$ . The discrete TF domain gain is  $\mathbf{H}_{\text{tf}} \in \mathbb{C}^{M \times N}$  with elements  $h(m, n)$  where  $m$  is the subcarrier index (frequency) from a set of  $M$  subcarriers of bandwidth  $\Delta f$  Hz and  $n$  is the symbol index (time) from a sequence of  $N$  OFDM symbols with period  $T$  seconds and  $T\Delta f = 1$ . Fig. 3a shows the channel response in the TF domain of a three-tap scattering channel with two scatterers moving at  $-337$  kph and  $540$  kph relative to the TA. The channel changes from symbol to symbol, meaning there is very little coherence time.

OFDM transmits a data grid  $\mathbf{X}_{\text{tf}} \in \mathbb{C}^{M \times N}$  where each grid element is called a *Resource Element* (RE) containing a data symbol from a QAM alphabet. The TF input-output relationship of  $\mathbf{H}_{\text{tf}}$  with  $\mathbf{X}_{\text{tf}}$  is the Hadamard (element-by-element) product such that the channel output  $\mathbf{Y}_{\text{tf}} \in \mathbb{C}^{M \times N}$  is

$$\mathbf{Y}_{\text{tf}}[m, n] = \mathbf{H}_{\text{tf}}[m, n]\mathbf{X}_{\text{tf}}[m, n]. \quad (1)$$

### B. The Delay-Doppler Channel Representation

The channel may also be described in the delay-Doppler domain, where the complex gain  $h(\tau, \nu)$  describes the DD domain channel gain of a scatterer path  $i$  at tap delay  $\tau_i$  and Doppler shift  $\nu_i$ . If only  $P$  paths exist, the two-dimensional delay-Doppler channel response is

$$h(\tau, \nu) = \sum_{i=0}^{P-1} h_i \delta(\tau - \tau_i) \delta(\nu - \nu_i). \quad (2)$$

The delay  $\tau_i$  is the delay relative to the first (LOS) tap. There is no time-dependent parameter  $t$  since it is assumed that the delay and Doppler channel parameters are quasi-stationary. Whereas the TF channel response  $\mathbf{H}_{\text{tf}}$  requires  $MN$  elements to describe the channel, the DD channel response in (2) only requires  $P$  non-zero elements to fully describe the channel.

Let the discrete DD channel response be  $\mathbf{H}_{\text{dd}} \in \mathbb{C}^{M \times N}$  where  $M$  is the number of delay bins,  $N$  is the number of Doppler bins, and the array indices are the delay index  $m$  and the Doppler index  $n$ . Referring back to fig. 3a, the TF channel representation of the doubly-selective channel is clearly non-uniform and non-stationary. Fig. 3b shows the DD channel representation where the response is not only stationary but also sparse. Each non-zero entry in the delay-Doppler response represents the delay of a path relative to the LOS path (represented as zero delay) and the Doppler shift (where the center of the axis is zero Doppler). The magnitude of the complex-valued path gain is the height of the peak.

The discrete DD data grid  $\mathbf{X}_{\text{dd}} \in \mathbb{C}^{M \times N}$  shown in fig. 4 is a grid of  $M$  delay bins by  $N$  Doppler bins comprising an array of QAM symbols like OFDM. An OTFS symbol comprises the  $M \times N$  REs, while an OTFS block comprises a column of  $M$  REs. The delay bin resolution is  $1/(M\Delta f)$  seconds and the Doppler bin resolution is  $1/NT$  Hz. For ease of exposition, we assume the  $i$ -th

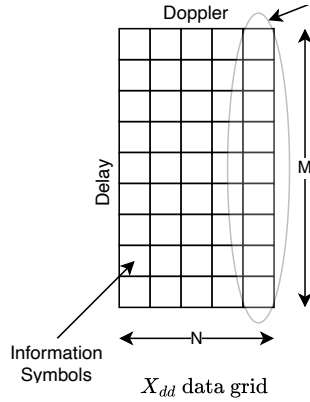


Figure 4: OTFS domain grid consisting of  $MN$  resource elements.

path delay  $\tau_i$  and Doppler  $\nu_i$  are multiples of the respective bin spacing such that  $\{l_i \in \mathbb{Z} | l_i = \tau_i/M\Delta f\}$  is the normalized delay index and  $\{k_i \in \mathbb{Z} | k_i = \nu_i/NT\}$  is the normalized Doppler index.

It is generally accepted that sampling rates in wideband systems are sufficiently high enough to ignore fractional normalized delays and that the observed path delays sufficiently approximate the actual path delays. Doppler shifts that are fractions of the Doppler bin spacing are called *fractional Doppler* and result in spreading of the response across adjacent Doppler bins.

The DD input-output relationship of the DD channel matrix  $\mathbf{H}_{\text{dd}}$  with  $\mathbf{X}_{\text{dd}}$  using ideal pulse shaping is a 2-D circular convolution such that the channel output  $\mathbf{Y}_{\text{dd}} \in \mathbb{C}^{M \times N}$  is

$$\mathbf{Y}_{\text{dd}}[m, n] = \mathbf{H}_{\text{dd}}[m, n] \circledast \mathbf{X}_{\text{dd}}[m, n] = \sum_{i=0}^{P-1} h_i \mathbf{X}_{\text{dd}}[|m - l_i|_M, |n - k_i|_N]. \quad (3)$$

The advantages of operating in the delay-Doppler domain are summarized as follows:

**Stationarity:** The channel response is quasi-stationary since the channel parameters of scatterer delay and Doppler change slowly over time. This means that CSI estimates have a longer lifespan

and channel estimation is performed less frequently as that done in the TF case. SE is improved as a result of the lower estimation overhead.

**Separability:** The problems of ICI and delay spread do not exist in the delay-Doppler domain because paths with different Doppler and delays are distinct/separable in the DD domain.

**Sparsity:** Describing the channel in the TF domain requires knowing the gains of  $MN$  elements, while the DD domain only requires knowing  $P$  elements. The sparsity of the channel response is ideal for CSI feedback compression and novel receiver architectures.

**Interpretability:** The channel response in the DD domain maps directly back to the physical environment. This lends itself well to the new field of Integrated Sensing and Communications (ISAC) where the physical parameters of transceivers and scatterers such as range and speed can be exploited for more efficient transmissions [10].

**Diversity:** Symbols in the DD domain are spread across time and frequency. When combined with channel coding, data is resistant to jamming in both frequency and time domains.

## DELAY-DOPPLER COMMUNICATIONS USING OTFS

Various modulations can implement communications in the DD domain, but OTFS has received the most attention in research literature. For space considerations, we refer many of the fundamentals of OTFS modulation, delay-Doppler channel description, and demodulation to [8] [11] [12]. We describe the system model here for completeness.

We assume that the transmitter and receiver in the system model are frame-synchronized, such that the first sample of the main line-of-sight (LOS) path is the first sample in the received signal vector. In other words, the LOS path arrives in the first delay bin.

### C. System Model

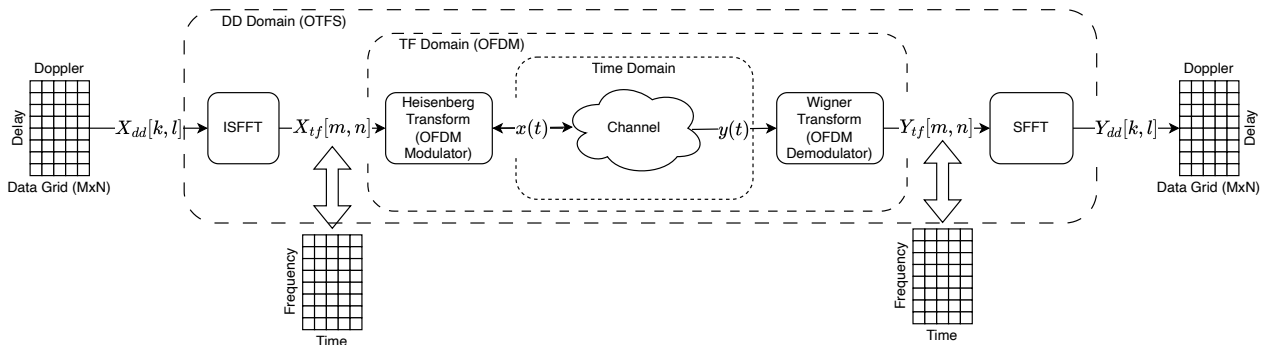


Figure 5: OTFS block diagram.

The OTFS system model is shown in fig. 5. Data is populated in the grid similar to filling  $N$  OFDM

symbols of length  $M$ .

#### D. Transmitter

The DD domain is transformed into the familiar TF domain by way of the Inverse Symplectic Finite Fourier Transform (ISFFT) block such that

$$\mathbf{X}_{\text{tf}}[m, n] = \frac{1}{MN} \sum_{k=0}^{M-1} \sum_{l=0}^{N-1} \mathbf{X}_{\text{dd}}[k, l] e^{j2\pi(\frac{nk}{N} - \frac{ml}{M})} \quad (4)$$

where  $\mathbf{X}_{\text{tf}}$  is the TF domain representation of  $\mathbf{X}_{\text{dd}}$ . Note the inner summation is simply performing an IDFT on each row of the DD grid, and the outer summation is performing a DFT on each column. Intuitively, the IDFT operation across the Doppler axis spreads each RE across time, which helps combat temporal fading.

Next, the Heisenberg transform operates on  $\mathbf{X}_{\text{tf}}$  to convert to time domain samples, and is equivalent to an OFDM modulator when rectangular pulse shaping is used. It is easy to see in this case that OTFS can be considered as block precoding of OFDM.

#### E. Receiver

The receiver is simply the inverse of the transmitter. Assuming rectangular pulse shaping, the Wigner transform is simply an OFDM demodulator that converts the received time domain signal into the 2-D TF signal  $\mathbf{Y}_{\text{tf}}$ . The “precoding” operation of the ISFFT is “combined” using the SFFT in the receiver following OFDM demodulation to bring the signal back into the DD domain as  $\mathbf{Y}_{\text{dd}}$ ,

$$\mathbf{Y}_{\text{dd}}[k, l] = \sum_{n=0}^{N-1} \sum_{m=0}^{M-1} \mathbf{Y}_{\text{tf}}[m, n] e^{-j2\pi(\frac{nk}{N} - \frac{ml}{M})}. \quad (5)$$

Again, the SFFT simply reverses the ISFFT and performs a DFT on each row and IDFT on each column of the received TF grid.

#### F. Decoding

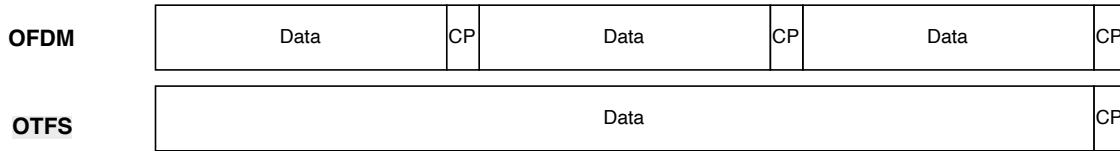
Various OTFS decoding schemes may be used to decode  $\mathbf{Y}_{\text{dd}}$  to produce the estimated transmit data sequence  $\hat{\mathbf{X}}_{\text{dd}}$ . Many algorithms leverage the sparsity of the DD channel to efficiently decode data, including message passing [13], LMMSE decoding [14], and maximal ratio combining (MRC) with successive interference cancellation (SIC) [15]. For this paper we use MRC-SIC for simulations.

## OTFS ADVANTAGES

In addition to the advantages operating in the delay-Doppler domain as outlined in section B., OTFS modulation has advantages over OFDM.

**Lower Inter-Symbol Interference Overhead:** Inter-Symbol Interference (ISI) is the contamination of adjacent symbols in time due to the channel delay spread. In OFDM, ISI is mitigated by separating each symbol of sample length  $M$  by a number of “throwaway” samples called a cyclic prefix (CP). The CP length  $M_{cp}$  is typically some fraction of  $M$  (usually 1/8 or 1/16) and is large enough such that the symbol smearing does not reach the next symbol. The CP adds no new information, so the CP is overhead that reduces the SE of the transmission system. Consequently it is desired to keep the CP as small as possible.

In OTFS, the CP is also added after each symbol, but OTFS symbols are of length  $MN$ . Therefore the ratio of CP samples to data samples is smaller. The CP overhead of OFDM and OTFS is listed in table 1. The OTFS overhead is smaller than OFDM a factor of  $(MN + M_{cp}) / (M + M_{cp})$ . Higher values of  $N$  asymptotically decreases the OTFS CP overhead but does not affect the OFDM CP overhead.



Modulation	Total Number of Samples	Overhead
OFDM	$M + M_{cp}$	$M_{cp} / (M + M_{cp})$
OTFS	$MN + M_{cp}$	$M_{cp} / (MN + M_{cp})$

Table 1: CP overhead of OFDM and OTFS.

**Lower Peak to Average Power Ratio:** One of the main shortcomings of using OFDM in the AMT environment is the high PAPR, which consequently requires a power back off of around 12 dB to prevent the transmit signal from saturating the power amplifier and causing out of band emissions. Due to the power back off, OTFS and OFDM are less power-efficient than CPM waveforms that can operate near the saturation point of the power amplifiers.

OTFS has a lower PAPR than OFDM due to the ISFFT performing a precoding operation prior to OFDM modulation [16]. The PAPR of OTFS is approximately 1 dB less than OFDM for typical DD grid sizes (shown in fig. 6). Thus OTFS gains a 1 dB link advantage over OFDM. The PAPR can be further reduced via pilot insertion methods, but at the cost of computational complexity.

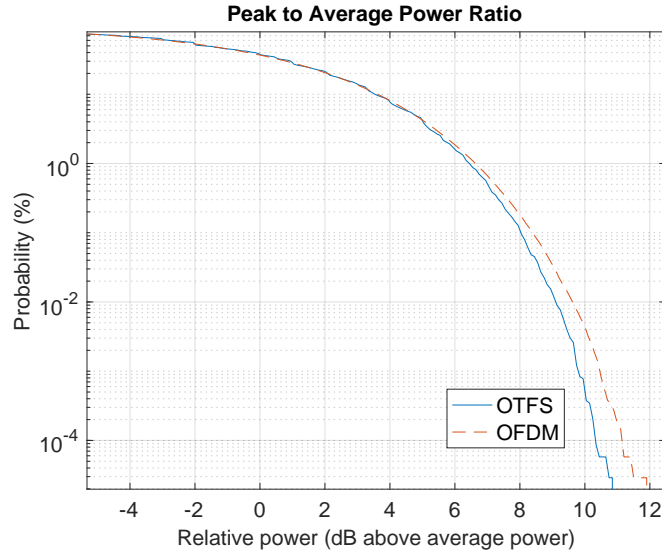


Figure 6: OFDM vs. OTFS PAPR,  $M=1024$ ,  $N=16$ .

### AMT SYSTEM DESIGN

To show the practicality of delay-Doppler communications for AMT, we formulate the OTFS parameters that can support an example high-velocity telemetry range. Consider a range telemetry system with the following requirements and constraints listed in table 2.

Category	Requirement
Small-scale Fading	Ricean fading with 1-2 scatterers [from [17] and [18]]
TA speeds	Up to Mach 2
Carrier frequency	S-band ( $f_c = 2.4$ GHz)
Bandwidth	15 MHz
Transmit power	25 Watts (IRIG-106 section 2.4.2)
Base station distances	60 km (as implemented in [2])

Table 2: Range telemetry system requirements and constraints.

The Doppler frequency is  $f_d = v f_c / c$  where  $f_c$  is the carrier frequency,  $v$  is the speed of the TA relative to the BS, and  $c$  is the speed of light. At  $f_c = 2.4$  GHz and a maximum aircraft speed of Mach 2 (2470 kph, or 686.1 m/s at sea level and 20 degrees Celsius), the Doppler frequency is 5490 Hz. Because the TA can approach or move away from a BS at Mach 2, the maximum supported Doppler of the receiver must be twice that, or 10980 Hz.

### G. OTFS Grid Size

We choose the grid size  $M \times N$  based on available bandwidth (for  $M$ ) and maximum allowable latency (for  $N$ ). A larger  $M$  increases throughput and allows for granularity in the delay domain.

The maximum supported Doppler (influenced by  $\Delta f$ ) and maximum supported delay spread (influenced by  $T$ ) are coupled by the relationship  $T\Delta f = 1$ . In the case of AMT, the maximum supported Doppler is a primary constraint and thus  $\Delta f$  is the primary driver of the OTFS grid design, with the supported delay spread being the dependent parameter.

The subcarrier spacing  $\Delta f$  must be at least 10980 Hz to support the anticipated Doppler range. We can use LTE's  $f_c = 15$  kHz subcarrier spacing, but this shortens the symbol period  $T$  and hence shortens the supported delay spread of the system. For now, we let the subcarrier spacing be 12 kHz. With the given 15 MHz bandwidth constraint, we can use  $M=1024$  subcarriers to occupy 12.28 MHz, which should be sufficient for spectral leakage containment at the band edges. With  $\Delta f$  set, we compute the delay grid resolution as  $T_{\text{res}} = 1/(12\text{kHz} * 1024) = 81.4$  ns or 24.4 m of propagation distance (80 ns is approximately the delay from a ground reflection to an elevated ground antenna [18]). This also means that the maximum scatterer delay is  $1/(12 \text{ kHz}) = 83.3 \mu\text{s}$ , or 25 km of propagation distance.

The choice of  $N$  is generally limited by any latency requirements, since each OTFS symbol must collect  $N$  subsymbols before demodulation can occur. However, higher values of  $N$  allow for more Doppler grid resolution. For this paper, we arbitrarily choose a value of  $N = 50$ , so the duration of each OTFS symbol without cyclic prefix is  $NT = 4.2\text{ms}$ . The Doppler grid resolution is  $12 \text{ kHz} / 50 = 600 \text{ Hz}$ , or velocity increments of 270 kph at 2.4 GHz.

With  $1024 \times 50 = 51200$  REs and  $\Delta f$  of 12 kHz, the bitrate is 2.476 Mbps using QPSK in each RE. With a CP length of  $M_{\text{cp}} = 64$ , the SE is  $(1024 * 50)/((1024 * 50) + 64) = 99.88\%$  or 2.455 Mbps. If OFDM were used, the SE would be  $1024/(1024 + 64) = 94.12\%$  or 2.313 Mbps.

### H. Delay-Doppler Coherence Time

We introduce a *DD coherence time* defined as the duration that a DD channel remains stationary in a mobile environment. At a high-level it is the amount of time that changes in propagation delays induce an appreciable change in the delay domain channel response. We wish to compute how many OTFS symbols can be transmitted during the coherence time before the channel must be estimated again. Recall that channel estimation is overhead that reduces the spectral efficiency of the system, so we wish to estimate as infrequently as possible.

In the span of one delay grid unit, the signal travels a distance of  $x_{\text{res}} = cT_{\text{res}}$ . The time it takes for a TA to travel that distance (and change the DD channel response to the next delay bin) would therefore be the DD coherence time  $T_{\text{coh}} = x_{\text{res}}/v = c/(\nu M\Delta f)$ . For a TA moving at Mach 2 (686 m/s), a DD grid with  $M = 1024$  and  $\Delta f = 12$  kHz would yield a DD coherence time of 35.5 ms. The channel in the DD domain is stationary for approximately  $35.5/4.2 \approx 8$  OTFS symbols before the channel would need to be estimated again.

When  $M$  is large relative to  $N$ , Doppler changes from a maneuvering TA don't affect DD coherence time. To show this, consider that the Doppler resolution in this example is 600 Hz or 270 kph as stated earlier. To change the Doppler response by even 10% of the Doppler resolution would require a  $270 \times 10\% = 27$  kph change in speed over 35.5 ms (the DD coherence time), or an unrealistic acceleration of 760 kph per second.

## SIMULATION

In this simulation, we show that OTFS can operate in a high-Doppler environment while OFDM suffers high bit errors. To isolate performance differences to just Doppler and timing effects, we assume perfect knowledge of the channel. We specifically focus on simulating a Single Frequency Network (SFN) architecture as described by 3GPP (Annex B.3.2 in [19]) that is favorable for an AMT range. An SFN eliminates cell-to-cell handovers by having all BS antennas transmit and receive the same data simultaneously to maintain continuous connectivity throughout the telemetry range without the interruptions inherent in traditional handovers or neighbor cell measurements.

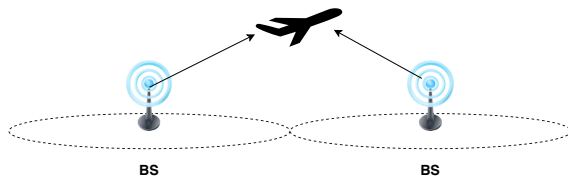


Figure 7: An SFN-based telemetry range with a TA at the cell edge.

Fig. 7 shows two BS antennas in an SFN transmitting the same data simultaneously to a TA at the cell edge. The TA combines the two signals but each has different Doppler shifts. Cell edge performance is a challenging use case because of low signal power and large interference from neighbor cells. The TA is traveling away from one BS at Mach 2 with a Doppler shift of -5490 Hz and traveling towards another BS with +5490 Hz of Doppler shift, so the net Doppler is 10980 Hz. When the TA is halfway between the two BS antennas, the signals arrive at exactly the same time (“perfect” timing) with the same power but with different Doppler shifts so ICI is expected. If the TA is closer to one BS than another, the signals arrive at slightly different times (“imperfect” timing), and the combined signal resembles a multipath signal with ICI.

Fig. 8 shows the uncoded BER for the described scenario. The SNR is 13.5 dB which is the expected free-space SNR at 30 km and transmitting at 2.4 GHz over 12.28 MHz of bandwidth. For OTFS, performance is the same across all TA speeds and whether the timing is perfect or imperfect. This shows how OTFS is unaffected by timing (due to the separable delay bins) and Doppler (due to the separable Doppler bins).

For OFDM with perfect timing, no bit errors occur when the TA is stationary because no ICI exists. Both signals arrive with constructive interference so the signal is stronger. This is clearly an outlier case since perfect timing is rarely possible. However, as speed increases, Doppler increases and the effect of ICI is seen in OFDM as increased bit errors. OFDM performance worsens as the

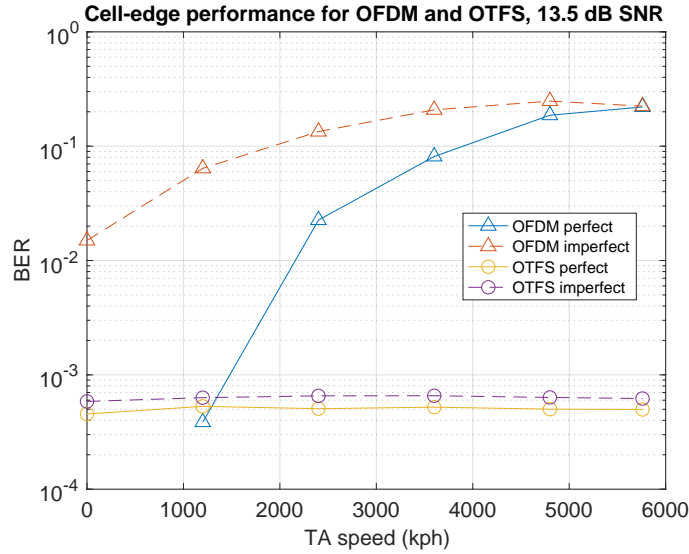


Figure 8: Cell-edge BER for OFDM and OTFS.

Doppler shift approaches the subcarrier bandwidth. When timing is imperfect, OFDM bit errors are predominantly due to subcarrier attenuation from frequency-selective fading, and ICI is less of a factor.

## OPEN CHALLENGES OF DELAY-DOPPLER COMMUNICATIONS IN AMT

OTFS research initially used 3GPP channel models representing terrestrial use cases such as pedestrian, vehicular, and HST scenarios. There are still open research areas in reducing receiver complexity and efficiently multiplexing users in the DD domain. However, new use cases are being developed to recognize higher speeds and deployments in large geographic areas that increase delay spread [19]. This section addresses these two areas of research for wide-area communication networks that address problems for multicarrier modulation schemes such as OFDM and OTFS.

**Fractional Doppler:** Fractional Doppler occurs when the Doppler value is not an integer multiple of  $1/M\Delta f$ . This results in a sinc-like path response that bleeds into adjacent Doppler bins. The channel response is not as sparse, and grid-based receiver algorithms need to process more low-SNR paths.

**Large Delay Spreads in AMT:** Channel estimation methods for OTFS assume that the delay spread is a small percentage (less than 15%) of the symbol time. For B5G and 6G, 3GPP has recognized that large delay spreads can exist in macrocells for wide-area deployments (similar to the AMT environment), and when subcarrier bandwidths increase (which leads to smaller symbol times).

Allocating a small sounding area is necessary for channel measurements but sacrifices SE. In large

delay spread channels, this method is no longer efficient. Thus new channel estimation techniques are needed that can measure large delay spread channels without sacrificing spectral efficiency.

**Pulse Shaping:** Novel pulse shapes may be needed to contain spectral leakage if OTFS were to co-exist with OFDM or other modulations.

## CONCLUSION

We presented the paradigm of delay-Doppler communications as a promising domain for high Doppler multi-path channels to support future AMT needs. OTFS is a precoded OFDM system that offers resistance to Doppler-induced interference and signal jamming, lower PAPR, and higher spectral efficiency from reduced cyclic prefix and channel estimation overhead than OFDM. We presented system parameters that can meet the needs of a telemetry range that supports a TA flying up to Mach 2, and showed the performance advantages of OTFS vs. OFDM in this unique environment. Finally, we listed challenges unique to AMT that provide open research topics.

## REFERENCES

- [1] C. Kahn, "Report to Congress on Aeronautical Mobile Telemetry," Tech. Rep. MP120385, MITRE, July 2014.
- [2] A. Krishnamoorthy, "Use of LTE for Cellular Range Telemetry (CRTM): A Simulation Study," in *International Telemetry Conference Proceedings*, vol. 53, (Las Vegas, NV), Oct. 2017.
- [3] A. Kogiantis, K. Rege, and A. A. Triolo, "LTE System Architecture for Coverage and Doppler Reduction in Range Telemetry," in *International Telemetry Conference Proceedings*, vol. 53, (Las Vegas, NV), Oct. 2017.
- [4] E. Fung, W. H. Johnson, A. Kogiantis, and K. M. Rege, "Doppler Estimation and Compensation for LTE-based Aeronautical Mobile Telemetry," in *International Telemetry Conference Proceedings*, vol. 54, (Glendale, AZ), Nov. 2018.
- [5] E. Beck, S. Erramilli, S. Habiby, W. Johnson, A. Kogiantis, N. Maung, K. Rege, Z. Sayeed, A. Triolo, and J. Young, "LTE-based Aeronautical Mobile Telemetry - Lab and Field Test Experiments," in *International Telemetry Conference Proceedings*, vol. 55, (Las Vegas, NV), Oct. 2019.
- [6] E. Beck, S. Erramilli, W. H. Johnson, A. Kogiantis, J. Maung, K. Rege, A. A. Triolo, and J. Young, "Cellular 4G LTE Aeronautical Mobile Telemetry Flight Test Results," in *International Telemetry Conference Proceedings*, vol. 56, (Las Vegas, NV), Oct. 2021.
- [7] V. Hedge, "Seamless Handover at High Speeds for Cellular Range Telemetry," in *International Telemetry Conference Proceedings*, vol. 53, (Las Vegas, NV), Oct. 2017.

- [8] R. Hadani, S. Rakib, M. Tsatsanis, A. Monk, A. J. Goldsmith, A. F. Molisch, and R. Calderbank, "Orthogonal Time Frequency Space Modulation," in *2017 IEEE Wireless Communications and Networking Conference (WCNC)*, pp. 1–6, 2017.
- [9] T. Wang, J. Proakis, E. Masry, and J. Zeidler, "Performance degradation of ofdm systems due to doppler spreading," *IEEE Transactions on Wireless Communications*, vol. 5, no. 6, pp. 1422–1432, 2006.
- [10] W. Yuan, L. Zhou, S. K. Dehkordi, S. Li, P. Fan, G. Caire, and H. V. Poor, "From OTFS to DD-ISAC: Integrating sensing and communications in the delay doppler domain," *IEEE Wireless Communications*, vol. 31, no. 6, pp. 152–160, 2024.
- [11] Y. Hong, T. Thaj, and E. Viterbo, *Delay-Doppler Communications: Principles and Applications*. Academic Press, 2022.
- [12] Z. Wei, W. Yuan, S. Li, J. Yuan, G. Bharatula, R. Hadani, and L. Hanzo, "Orthogonal Time-Frequency Space Modulation: A Promising Next-Generation Waveform," *IEEE Wireless Communications*, vol. 28, no. 4, pp. 136–144, 2021.
- [13] P. Raviteja, K. T. Phan, Y. Hong, and E. Viterbo, "Interference cancellation and iterative detection for orthogonal time frequency space modulation," *IEEE Transactions on Wireless Communications*, vol. 17, no. 10, pp. 6501–6515, 2018.
- [14] S. Tiwari, S. S. Das, and V. Rangamgari, "Low complexity LMMSE receiver for OTFS," *IEEE Communications Letters*, vol. 23, no. 12, pp. 2205–2209, 2019.
- [15] T. Thaj and E. Viterbo, "Low complexity iterative rake decision feedback equalizer for zero-padded OTFS systems," *IEEE Transactions on Vehicular Technology*, vol. 69, no. 12, pp. 15606–15622, 2020.
- [16] G. D. Surabhi, R. M. Augustine, and A. Chockalingam, "Peak-to-Average Power Ratio of OTFS Modulation," *IEEE Communications Letters*, vol. 23, no. 6, pp. 999–1002, 2019.
- [17] E. Haas, "Aeronautical Channel Modeling," *IEEE Transactions on Vehicular Technology*, vol. 51, no. 2, pp. 254–264, 2002.
- [18] M. Rice, A. Davis, and C. Bettweiser, "Wideband Channel Model for Aeronautical Telemetry," *IEEE Transactions on Aerospace and Electronic Systems*, vol. 40, no. 1, pp. 57–69, 2004.
- [19] 3GPP, "Radio Access Network; NR; Base Station (BS) radio transmission and reception," Technical Specification (TS) 38.101, 3rd Generation Partnership Project (3GPP), 2025. Version 19.1.0.